The Astronomical Journal, 134:579–593, 2007 August

A CATALOG OF MORPHOLOGICALLY CLASSIFIED GALAXIES FROM THE SLOAN DIGITAL SKY SURVEY: NORTH EQUATORIAL REGION

Masataka Fukugita,[1,2] Osamu Nakamura,[3] Sadanori Okamura,[4] Naoki Yasuda,[1] John C. Barentine,[5] Jon Brinkmann,[5] James E. Gunn,[6] Mike Harvanek,[5] Takashi Ichikawa,[7] Robert H. Lupton,[6] Donald P. Schneider,[8] Michael A. Strauss,[5] and Donald G. York[9]

Received 2006 June 20; accepted 2007 April 11

ABSTRACT

We present a catalog of morphologically classified bright galaxies in the north equatorial stripe (230 deg^2) derived from the Third Data Release of the Sloan Digital Sky Survey (SDSS). Morphological classification is performed by visual inspection of images in the *g* band. The catalog contains 2253 galaxies complete to a magnitude limit of $r = 16$ after Galactic extinction correction, selected from 2658 objects that are judged to be extended in the photometric catalog in the same magnitude limit. A total of 1866 galaxies in our catalog have spectroscopic information. A brief statistical analysis is presented for the frequency of morphological types and mean colors in the catalog. A visual inspection of the images reveals that the rate of interacting galaxies in the local universe is approximately 1.5% in the $r \leq 16$ sample. A verification is made for the photometric catalog generated by the SDSS, especially as to its bright-end completeness.

Key words: catalogs — galaxies: fundamental parameters

Online material: machine-readable table

1. INTRODUCTION

This paper presents a catalog of morphologically classified galaxies from the Sloan Digital Sky Survey (SDSS; York et al. 2000) Data Release Three (DR3; Abazajian et al. 2005). We limit our sample to a rectangular region of the equatorial area in the northern sky (R.A. $\approx 9.7^{\rm h}$–$15.7^{\rm h}$) of 230 deg^2 that comprises 2658 objects brighter than the *r*-band Petrosian magnitude $r_{\rm P} \leq 16$ that are listed as extended in the DR3 photometric catalog. The classification is performed by visual inspection by three people independently, and the final classification is obtained from the mean. We obtain a sample of 2253 galaxies, of which 1866 have spectroscopic information in the SDSS.

Visual classification is a laborious and somewhat subjective procedure. Nevertheless, this remains the best approach for classifying each galaxy into a Hubble type with high confidence, at least for bright galaxies. There are a number of methods that use photometric and/or spectroscopic parameters developed for large-scale samples to classify galaxies. Those classifications are correlated reasonably well with visual Hubble types but are substantially contaminated by galaxies that belong to obviously wrong classes if visual inspection is made. The identification of Sa galaxies is particularly subtle. The classification of Sa galaxies often scatters across elliptical to late spiral galaxies, if one uses photometric and/or spectroscopic parameters as indicators. On the other hand, it is not difficult to identify disks of Sa galaxies with visual inspection. Color or spectroscopic parameters are sensitive to star formation activity, so galaxies that show such activities are typically classified as late type if those parameters are used. For the moment it is difficult to replace the classification with a quantitative measure.

Our work follows the traditional line of the Revised Shapley Ames Catalogue (Sandage & Tammann 1980), the Reference Catalogue of Bright Galaxies (de Vaucouleurs & de Vaucouleurs 1964; de Vaucouleurs et al. 1995, hereafter RC3), the Uppsala General Catalogue of Galaxies (Nilson 1973), and several others (e.g., Marzke et al. 1994; Kochanek et al. 2001; see also Blanton et al. [2005] and Driver et al. [2006], who carried out rudimentary visual classifications). The size of our sample is moderate, but it is based on photometric criteria accurate enough to define the basic catalog, and it provides a photometrically homogeneous sample that can be used for a variety of galaxy studies. We have endeavored to alleviate the subjectivity of visual classification by taking a mean of three independent classifiers.

This catalog also allows us to verify the quality of the SDSS photometric catalog at the bright end. Definite photometric criteria are applied to produce a galaxy sample that is to be targeted for spectroscopic observations (Strauss et al. 2002). The problem is that we are not able to produce a genuine galaxy catalog with simple numerical criteria. The catalog obtained may thus contain objects that are not genuine galaxies, such as double stars, stars with somewhat deformed images, ghosts, satellite images, and "shredded" objects (caused by failures in deblending of large bright galaxies). On the contrary, an application of stricter criteria would miss many true galaxies, so a compromise is needed. We visually inspect all objects that are selected with a rather loose criterion for extended objects, which permits quantification of the contamination and completeness of the photometric catalog produced by the SDSS target selection on the bright end.

We also give a subsidiary catalog of $r'_{\rm P} \leq 15.9$ galaxies that were contained in the Early Data Release (EDR; Stoughton et al. 2002), since a number of scientific publications (Nakamura et al.

[1] Institute for Cosmic Ray Research, University of Tokyo, Kashiwa 277 8582, Japan.
[2] Institute for Advanced Study, Princeton, NJ 08540, USA.
[3] Graduate School of Political Science, Waseda University, Shinjiku, Tokyo 169 8050, Japan.
[4] Department of Astronomy, University of Tokyo, Hongo, Tokyo 113, Japan.
[5] Apache Point Observatory, Sunspot, NM 88349, USA.
[6] Princeton University Observatory, Princeton University, Princeton, NJ 08544, USA.
[7] Astronomical Institute, Tohoku University, Sendai 980 8578, Japan.
[8] Department of Astronomy and Astrophysics, Pennsylvania State University, University Park, PA 16802, USA.
[9] Department of Astronomy and Astrophysics, University of Chicago, Chicago, IL 60637, USA.

TABLE 1
MORPHOLOGICAL INDEX T

Hubble Type	E	S0	Sa	Sb	Sc	Sd	Im	Unclassified
T(ours)	0	1	2	3	4	5	6	−1
T(RC3)	−6 to −4	−3 to −1	1	3	5	7–8	10	...

2003, 2004; Ohama 2003; Fukugita et al. 2004; Ball et al. 2004; Yamauchi et al. 2005; Tasca & White 2005) have used this earlier version of the morphologically classified galaxy catalog. Identification of all objects in both catalogs is also given. We note that the revision in the estimate of morphological type is small, if any, for individual galaxies, and the results given in the earlier papers will change little with the use of the present catalog.

We refer the reader to the other publications for detailed descriptions of the SDSS related to our study: Gunn et al. (2006) for the telescope, Gunn et al. (1998) for the photometric camera, Fukugita et al. (1996) for the photometric system, Hogg et al. (2001) and Smith et al. (2002) for external photometric calibrations, and Pier et al. (2003) for astrometric calibrations. We also refer to Abazajian et al. (2003, 2004) and Adelman-McCarthy et al. (2006) for other data releases from the SDSS, which discuss the successive improvement of the pipelines used to derive the basic catalogs.

2. PROCEDURES

Our rectangular region is defined by $145^\circ < \alpha(\mathrm{J2000.0}) < 236^\circ$ and $-1.26^\circ < \delta(\mathrm{J2000.0}) < 1.26^\circ$, covering an area of 230 deg^2. This area fully encompasses SDSS survey stripe 10, but the region of primary observations that takes account of overlaps between stripes is somewhat rounded toward its corners. So we supplement the missed part from neighboring stripes (stripes 9 and 11) to make the area strictly rectangular in celestial coordinates. We take photometry from DR3 and select all extended objects[10] that are brighter than Petrosian magnitude $r_{\mathrm{P}} = 16$ (see the EDR and Strauss et al. 2002 for the precise definition) after the Galactic extinction correction (Schlegel et al. 1998). There are 2658 such objects in the DR3 catalog that are produced from version 5.4 of the photometric pipeline.

We note that there are some gaps (0.03 deg^2 altogether) within the region that concerns us. There are five fields ($13.5' \times 9.0'$) for which the photometric pipeline did not process the data (the actual gap is somewhat smaller due to overlaps with adjacent fields). This happens when the field contains very bright galaxies or stars with conspicuous spikes and the completion of deblending required more time than the pipeline limit. Any galaxies located in these fields are not included in our sample.

All objects are visually inspected by three classifiers (M. F., O. N., S. O.) independently. This sample is contaminated by nongalactic objects. Our initial sample of 2658 objects includes a number of sources that are not galaxies (stars, satellite trails, or optical defects), as well as multiple entries for a single object (primarily due to deblending failures). Removal of these objects produces a final sample of 2253 galaxies.

Morphological classification is carried out in reference to the Hubble Atlas of Galaxies by Sandage (1961) by three classifiers using the SAOimage viewer. We use the monochromatic g-band image, which is similar to the commonly used B-band image for classification and is sensitive to H II regions and arm structures. It is important to inspect images with both linear and logarithmic scales in the viewer with varying contrast levels. This occasionally produces a systematic difference from classifications based on photographic materials. We intentionally avoid using color information so that morphology is solely determined by the appearance, as has been done traditionally. This allows us to consider the correlation between morphology and colors in an unbiased way.

We divide the classifications into seven classes, $T = 0$ (E), 1 (S0), 2 (Sa), 3 (Sb), 4 (Sc), 5 (Sd), and 6 (Im), allowing for half-integer classes. We do not adopt more detailed classes such as those defined in RC3 (which has 16 classes in T), since our experience with the SDSS data (comparing results from the three classifiers) is that a finer division is unwarranted. The Hubble Atlas does not define Sd and Sdm. We assign the latest of the Sc galaxies in the Hubble Atlas as Sd-Sdm so that our classification scheme matches with that in RC3. Irr I of the Hubble Atlas is denoted as Im in this paper, also in agreement with RC3. We assign $T = -1$ when we are unable to classify a galaxy into a conventional Hubble type. We indicate by a letter "p" when some peculiarity is noted in a galaxy (such as somewhat disturbed shapes, rings, or dust lanes, as in the Hubble Atlas) even though it can be classified into a regular, $T \neq -1$ Hubble type. The relations between our T and T(RC3) are shown in Table 1. We note slight biases in our classification toward integer T. We are not concerned with whether galaxies have bars or not.

During the classification we noticed that not all galaxies fell nicely into the Hubble sequence, but whenever possible we classify a galaxy into the $T = 0$–6 scale. This leads to a number of cases where the appearance of the galaxy may not match well with the appearance of the Hubble Atlas prototype, but we view this as preferable to a catalog containing a large number of unclassifiable ($T = -1$) objects. Our catalog contains 33 galaxies with $T = -1$.

We noted that some galaxies, notably among those with $T = -1$, show a common feature characterized by a high surface brightness and a smooth light distribution, but their appearance is definitely not that of E or S0 galaxies. These objects frequently have more irregular shapes than early-type galaxies, but the light distribution is too smooth and/or surface brightness too high to be classified as Im. They appear to be reminiscent of Irr II galaxies in the Hubble Atlas or the "amorphous" galaxies introduced by Sandage & Brucato (1979), who characterized them as "not E, S0, or any type of spiral no matter how peculiar, but rather [having] an amorphous appearance to the unresolved light." Gallagher & Hunter (1987) used the term amorphous to represent "all galaxies with E/S0-like morphologies whose other global properties resemble irregular galaxies." These definitions, however, are not quite clear. These galaxies tend to show a red color. We confirmed that most of the galaxies of this type in our sample show red colors, although we did not use the color information when we classified galaxies. We indicate by "am" when we encounter those galaxies, whether they are left unclassified or classified into regular types (see Fig. 10).

[10] Technically, the selection is made using flag `type` = 3 (galaxy), not `saturated`, and not `satur_center` for all color bands. Objects that are flagged as `type` = 3 and not `satur_center` but flagged as `saturated` are visually inspected and included in the catalog when appropriate.

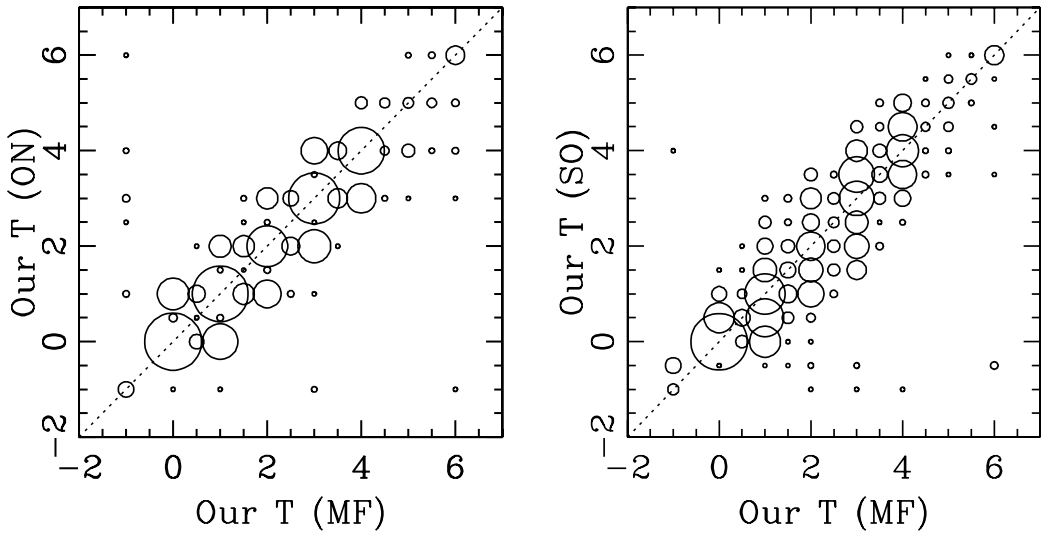

FIG. 1.—Correlation of visually inferred morphological types among three classifiers. The area of the circle represents the number of galaxies in the grid.

If the SDSS photometric pipeline determines that an image is actually composed of more than one component, the "parent" image is deblended into "child" images (Lupton 2006). The child images may be further deblended if they are judged to be formed of more than one component. When confronted with a large, complex surface brightness pattern, the deblender "shreds" a bright extended galaxy into a multitude of components, which can obviously affect the morphology of the galaxy (and also photometric measurements). (An extreme example is the separation of a nucleus, which may look like an S0, from a spiral galaxy.) For this reason it is important to inspect both parent and child images for all objects to ensure correct classifications.

Each classifier independently carries out the classification of each galaxy at least twice. The results are then compared, and when the results for an individual galaxy differ by more than 1.5 units in T all classifiers reinspect the galaxy in question and make a final, independent assessment. The adopted morphological classification is the mean of the measurements of the three classifiers.

The panels in Figure 1 display the correlation in T among the three classifiers. The dispersion is 0.4, or $\approx$1 in the RC3 T scale. This is probably as good as can be expected for visual classification; for example, $\delta T(\mathrm{RC3}) = 1.8$ in Lahav et al. (1995), a study that used photographic prints.

The final SDSS sample contains 218 galaxies that have an assigned T(RC3) in the RC3 catalog. Figure 2 shows the correlation of T(RC3) versus those from our classification for those common galaxies. The correlation is generally good; however, there is a systematic difference in the classifications in that S0/a–Sa(Sab) galaxies in RC3 are classified somewhat later, as Sa–Sb (occasionally as Sc), in our catalog. On the other hand, our E and S0 galaxy samples do not contain any galaxies that are classified as S0/a or later in RC3. We suspect the main reason for the discrepancy to be that our classification is based on high dynamic range and high-contrast CCD images, which allow detection of arm structure and detailed texture that would not be apparent in a single photometric image. This will drive our classification of disk galaxies toward later types compared to those in the RC3 catalog.

The quality of the photometry is also examined by visual inspection of images, to check whether the SDSS atlas image contains the entire image of the galaxy. If these data contain extra objects or parts of the galaxy are erroneously removed by the deblender, flags are attached. The position of the spectroscopic fiber, which has a diameter of 3″, is also inspected. When the fiber is not centered on the nucleus but is assigned to a region of the galaxy (e.g., a bright H II region), the spectroscopic information is accepted but flagged.

3. CATALOG

Table 2 presents our final catalog from DR3 ($r_{\mathrm{P}} \leq 16$) in order of right ascension, but only the top 20 lines are shown in the printed version of the paper. The entire catalog is available in the electronic edition of the *Astronomical Journal*. The catalog contains 15 columns with the following information:

Column (1): Catalog number.

Column (2): Photometric identification number in DR3. The numbers indicate run (observation)-camcol (camera column)-rerun (photometric data reduction)-field-object identification (see DR3 for details).

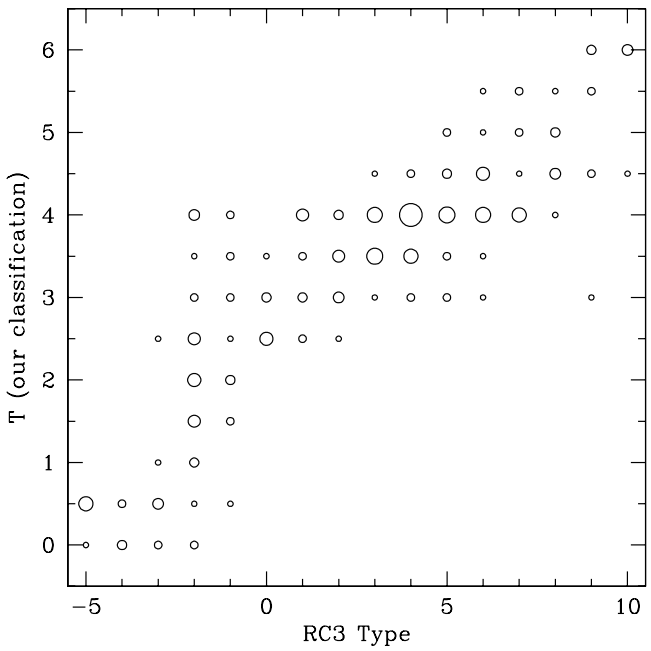

FIG. 2.—Correlation of our T with those of RC3 for 218 galaxies common to the two samples. The area of the circle represents the number of galaxies in the grid.

TABLE 2

CATALOG OF MORPHOLOGICALLY CLASSIFIED GALAXIES

ID (1)	DR3 Photo ID (2)	α (J2000.0) (3)	δ (J2000.0) (4)	EDR Photo ID (5)	$I_{\rm sample}$ (6)	$I_{\rm target}$ (7)	T (8)	$\sigma(T)$ (9)	$I_{\rm ph}$ (10)	$r_{\rm P}$ (11)	Spectro ID (12)	z (13)	CL(z) (14)	Remarks (15)
1.....	0756-6-44-0195-0158	145.00014	1.10623	...	2	2	0.5	0.4	0	15.64	477-52026-100	0.0605	0.999	
2.....	0756-4-44-0195-0158	145.04410	0.22011	...	2	2	3.0	0.0	0	15.49	476-52314-587	0.0621	0.998	
3.....	0756-4-44-0195-0165	145.04752	0.23774	...	2	2	1.0	0.4	0	15.25	476-52314-585	0.0622	0.999	
4.....	0756-5-44-0195-0208	145.06132	0.70924	...	2	2	3.5	0.5	0	15.61	477-52026-98	0.0260	0.958	
5.....	0756-4-44-0196-0172	145.22040	0.41082	756-4-8-0196-0174	3	2	3.5	0.6	0	15.89	266-51630-350	0.0982	1.000	
6.....	1239-1-40-0167-0166	145.37412	−1.24928	752-1-8-0012-0078	3	1	0.0	0.4	0	14.89	...	0.000	0.000	
7.....	0756-4-44-0198-0055	145.51373	0.33644	...	2	1	4.0	0.0	2p	11.77	...	0.000	0.000	PGC 2773
8.....	1239-2-40-0169-0142	145.64788	−0.77173	752-2-8-0014-0175	3	2	3.0	0.8	0	15.75	266-51630-215	0.0218	0.992	
9.....	0756-1-44-0199-0259	145.68110	−0.86723	756-1-8-0199-0148	3	2	2.0	0.5	0	15.60	266-51630-207	0.0676	0.999	
10.....	1239-2-40-0170-0139	145.75971	−0.81389	...	2	2	2.5	0.5	0	15.96	266-51630-216	0.0676	0.946	
11.....	1239-1-40-0170-0201	145.76792	−1.07472	752-1-8-0015-0167	3	1	3.5	0.5	0	15.84	...	0.000	0.000	
12.....	0756-4-44-0200-0098	145.80018	0.41417	756-4-8-0200-0158	3	2	4.0	0.4	0	14.18	266-51630-430	0.0252	0.996	PGC 27803
13.....	0756-5-44-0200-0211	145.84750	0.67573	756-5-8-0200-0131	3	2	2.5	0.5	0	15.87	266-51630-422	0.0266	1.000	
14.....	0756-6-44-0200-0100	145.85049	1.20353	756-6-8-0200-0063	3	2	1.5	0.5	0	15.60	480-51989-272	0.0618	1.000	
15.....	1239-4-40-0170-0202	145.87328	0.05683	752-4-8-0015-0058	3	1	1.0	0.4	0	15.88	...	0.000	0.000	
16.....	0756-2-44-0201-0130	145.87445	−0.60876	756-2-8-0201-0156	3	2	4.0	0.0	0	15.89	266-51630-138	0.0715	0.999	
17.....	0756-6-44-0201-0022	145.89254	1.11773	...	2	2	-1.0	0.0	0	15.93	480-51989-266	0.0512	0.986	int, am
18.....	1239-5-40-0171-0179	145.94781	0.46530	752-5-8-0016-0090	3	2	1.0	0.8	0	15.17	266-51630-467	0.0304	0.997	
19.....	1239-2-40-0171-0091	146.00780	−0.64227	752-2-8-0016-0100	3	2	-1.0	0.0	2p	15.89	266-51630-100	0.0051	0.938	
20.....	0756-5-44-0202-0018	146.02092	0.73355	756-5-8-0202-0009	3	2	0.5	0.6	0	14.10	266-51630-461	0.0362	0.999	

NOTES.—Units of right ascension and declination are decimal degrees. Table 2 is published in its entirety in the electronic edition of the *Astronomical Journal*. A portion is shown here for guidance regarding its form and content.

Column (3): Right ascension (J2000.0), in decimal degrees.

Column (4): Declination (J2000.0), in decimal degrees.

Column (5): Photometric identification number in EDR (see explanation for col. [2]).

Column (6): $I_{\rm sample}$ flag for catalog inclusions: (3) in both DR3 ($r_{\rm P} \leq 16$) and EDR ($r'_{\rm P} \leq 15.9$); (2) only in DR3 ($r_{\rm P} \leq 16$).

Column (7): $I_{\rm target}$ flag for spectroscopic target selection: (0) not targeted; (1) targeted but not observed; (2) observed; (2:) fiber positioned off-nucleus, but on some other part of the object carrying the specified photometric identification.

Column (8): Morphological index T: the mean of the three classifiers rounded to the nearest integer or half-integer.

Column (9): Standard deviation of morphological indices among the three classifiers.

Column (10): $I_{\rm ph}$ photometry quality: (0) good photometry (typical error expected to be smaller than approximately 0.1 mag based on visual estimates); (1) photometry is accurate if one uses the magnitude given to the parent image; (2) some errors, e.g., 0.3 mag (with visual estimates), suspected in photometry; (3) poor photometry. (Note that these flags are somewhat subjective.) Flags 2 and 3 are occasionally appended by p or c, which means that more accurate magnitudes may easily be obtained by applying aperture photometry centered on the designated object using parent or child atlas image frames, respectively.

Column (11): Petrosian r magnitude (of the child image) after correcting for Galactic extinction.

Column (12): Spectroscopic identification number: spectroscopic plate number-MJD-fiber number.

Column (13): Heliocentric redshift.

Column (14): Confidence level of redshift measurement.

Column (15): Remarks: "p" stands for peculiar, and this flag is given only when galaxies are classified into normal types; "am" is given to galaxies with an amorphous appearance; "int" stands for interacting, and "d-nucl" indicates double nuclei within a single galaxy. "Double" and "multiple" stand for more than one galaxy in the child field, while interactions among them are not apparent. The PGC number is provided when the galaxy is identified with that listed in RC3.

At the bottom of Table 2 we append a similar catalog for 22 objects that are included only in our EDR sample ($r'_{\rm P} \leq 15.9$). All of the galaxies have Galactic-extinction-corrected $r_{\rm P} > 16$ in DR3. This change from the EDR measurement is due to reprocessing the EDR data with the improved DR3 photometric pipeline. Flag (1) is assigned to column (6), "flag for catalog inclusions." We carried out reclassifications for the EDR sample, but the change compared to the earlier catalog is insignificant.

Figures 3–7 display examples of *gri* color synthetic images of galaxies (20 each) that are classified as $T = 0$–4, taken from the Catalog Archive Server. Figure 8 shows images for $T = 5$ (*top two rows*) and $T = 6$ (*bottom three rows*). Note that detailed textures are not quite visible on these pictures and the contrast is not always well represented, so that these printed images are not always appropriate for the purpose of classification. Figure 9 shows 12 galaxies that we classified as interacting; the four galaxies in the bottom row have double (multiple) nuclei. Figure 10 shows 16 galaxies to which we give amorphous ("am") flags. The size of the pictures are all $1' \times 1'$.

4. VERIFICATION OF THE PHOTOMETRIC CATALOG OF DR3

We have adopted a set of inclusive selection criteria so that few galaxies are missed in our initial sample. This selection is substantially looser than that adopted in the operational spectroscopic target selection for galaxies (Strauss et al. 2002).

Among the 2658 extended objects in our sample, 2253 are unique galaxies. There are 27 examples of galaxies that are included two or more times in the initial list; this primarily arises from deblending difficulties. Also included in our original set are 211 stars (approximately 80% of which are double stars) and 167 spurious objects, such as satellite trails, diffraction spikes of bright stars, ghosts, failures of deblending or of removal of bright stars that saturate the CCD, and empty fields with no designated object (which typically happens when images of the same fields with other color bands are hit by satellite trails). Nearly all stars (206 out of 211) can be rejected if one imposes the condition $g(\mathrm{PSF}) - g(\mathrm{model}) > 0.5$ for the selection of galaxies, which is tighter than the one used in target selection, $r(\mathrm{PSF}) - r(\mathrm{model}) > 0.3$. The former condition rejects six true galaxies (one among them looks like an AGN); 61 spurious objects, however, escape the rejection and contaminate the galaxy sample.

Among the 2253 galaxies, 2213 (98.2%) are chosen by SDSS target selection, and 1866 (82.8% of the entire galaxy sample) are actually spectroscopically observed.[11] The completeness of the spectroscopic observation in our sample is essentially uniform from early to late types. One reason for missing spectroscopy is the fiber-separation constraint (fibers on a given plate must be separated by at least 55″; Blanton et al. 2003a). In cases where a galaxy and a quasar candidate conflict, the fiber is assigned to the latter. We found a few patches for which spectroscopic observations were not carried out for unknown reasons. We also found that 168 more targets are set by target selection on nongalactic objects, of which 18 are observed.[12]

The survey samples are summarized in Table 3. The spectroscopic sample is quite clean even for bright galaxies of our sample, but with a completeness of 83%. We wish to inject a note of caution to the use of SDSS photometric galaxy catalogs. The target-selection algorithm of Strauss et al. (2002) yields a sample of galaxies with good completeness (only 2% of galaxies missed) but suffers a 7% contamination by stars and spurious objects.

In order to examine the statistical completeness, we show in Figure 11 the number of galaxies as a function of r magnitude. The solid line shows $N \sim 10^{0.6r}$, expected for Euclidean geometry. The data indicate that the galaxy number count deviates little from this line from 10 to 16 mag. A slight excess at bright magnitudes is consistent with the Poisson statistics. This implies that we have not missed too many galaxies even in the bright end of the sample at 10–10.5 mag. The spectroscopic sample is indicated by hatching, which shows that the spectroscopic completeness stays nearly constant for $r > 12.5$. The heavy hatching indicates galaxies that carry a flag for photometric errors, which increases toward brighter magnitudes, from 5% at $r = 15.5$ to 20% at $r = 13$. The number count for each morphological type is shown in Figure 12. All curves are consistent with $N \sim 10^{0.6r}$ up to statistical errors, indicating homogeneity in morphological compositions, and therefore morphological fractions change little as a function of magnitude to $r = 16$. We note, however, that the region considered has some overdensity at $z \sim 0.8$, where more

[11] Note that stripe 10 was observed in early days of the SDSS observation, when the tuning of spectroscopic observations was still immature. We suspect a higher rate of spectroscopic observations for stripes observed in later times.

[12] We suspect that these rather large numbers are likely due to deblending errors of the early immature version of the photometric pipeline used for spectroscopic target selection, since spectroscopic observations are carried out in the early stages of SDSS operations for the region that concerns us in this paper.

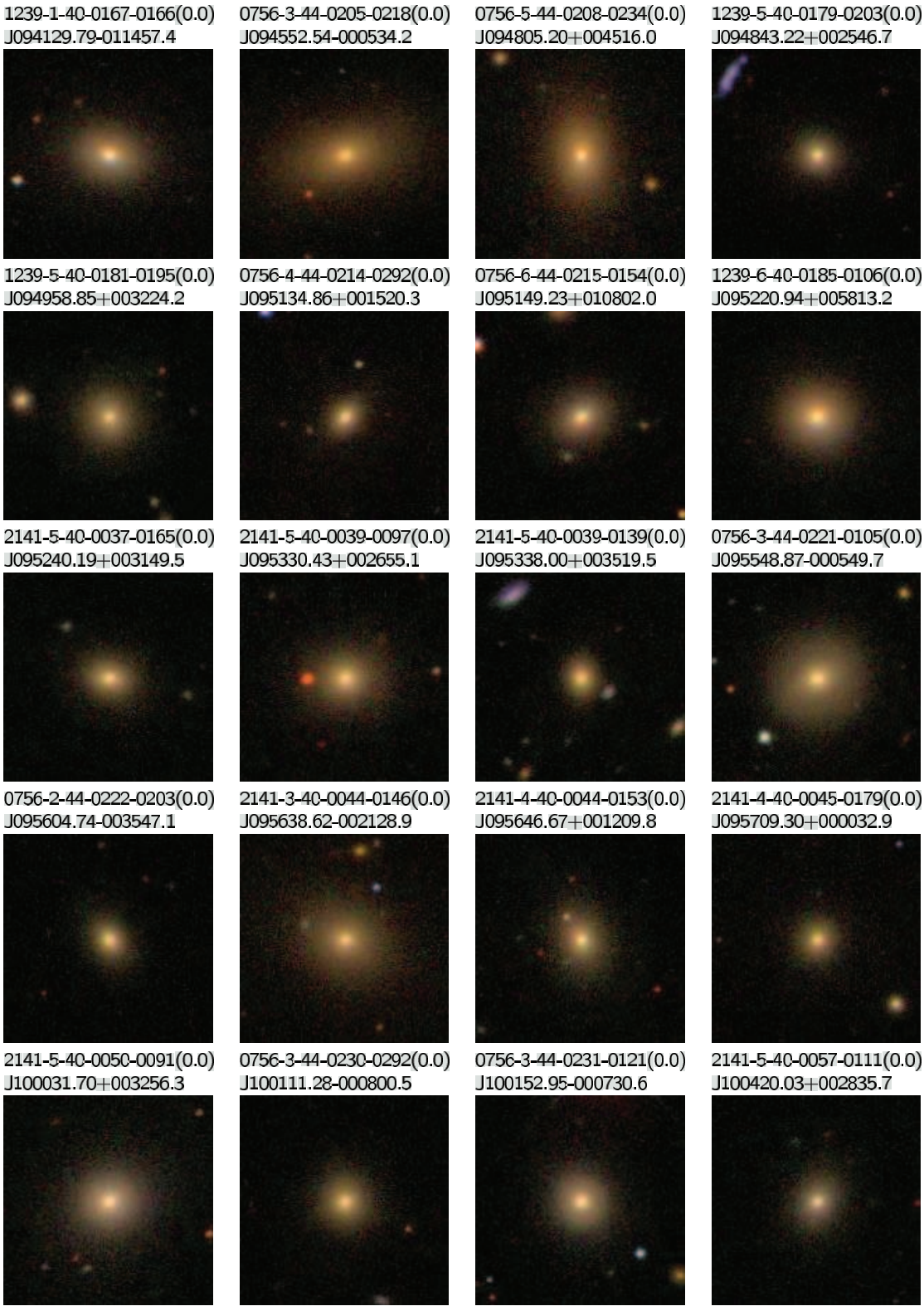

FIG. 3.—Sample of E ($T = 0$) galaxies with synthetic *gri* color. The size is $1' \times 1'$ for all pictures.

FIG. 4.—Sample of S0 ($T = 1$) galaxies. The format is the same as for Fig. 3.

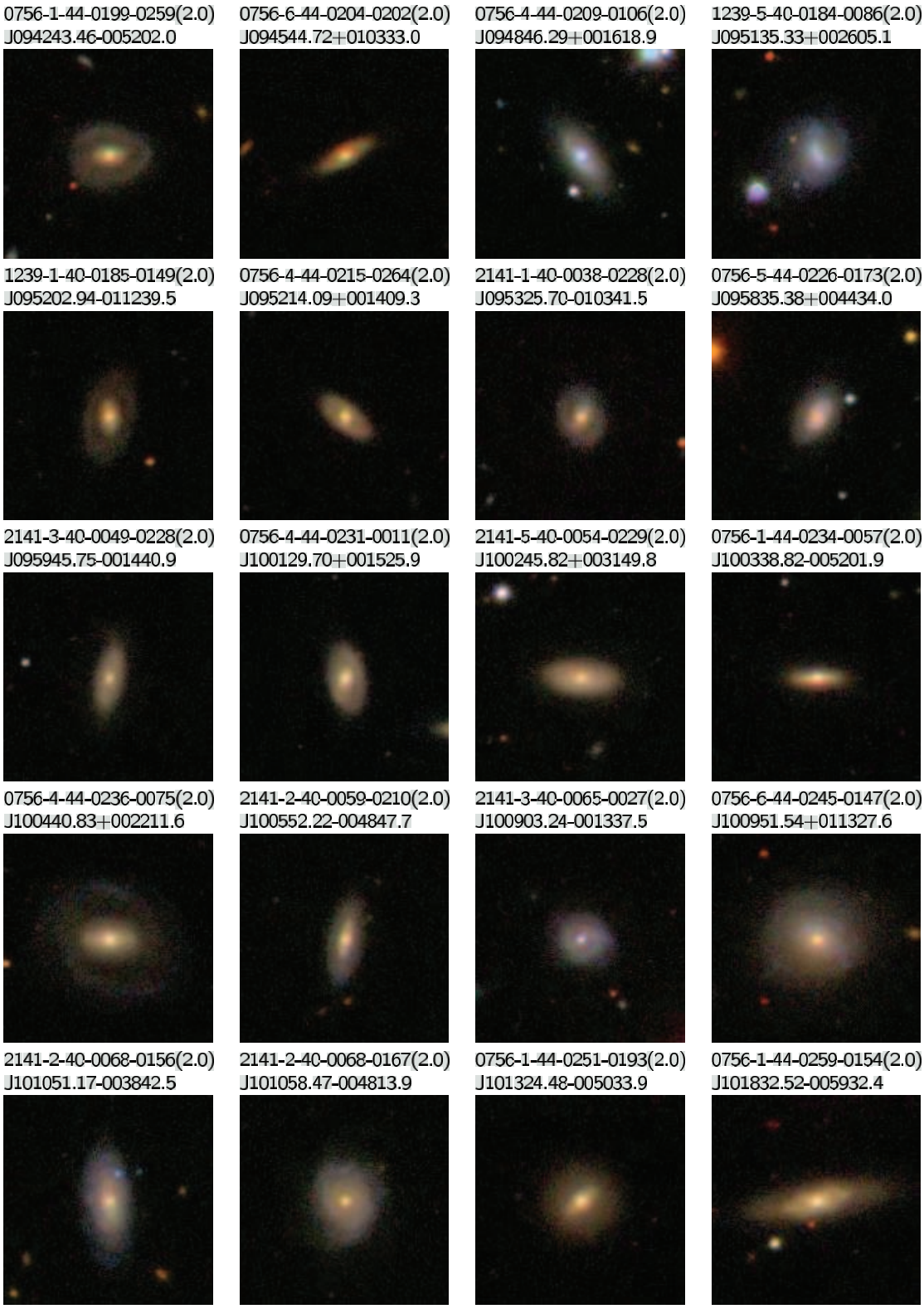

FIG. 5.—Sample of Sa ($T = 2$) galaxies. The format is the same as for Fig. 3.

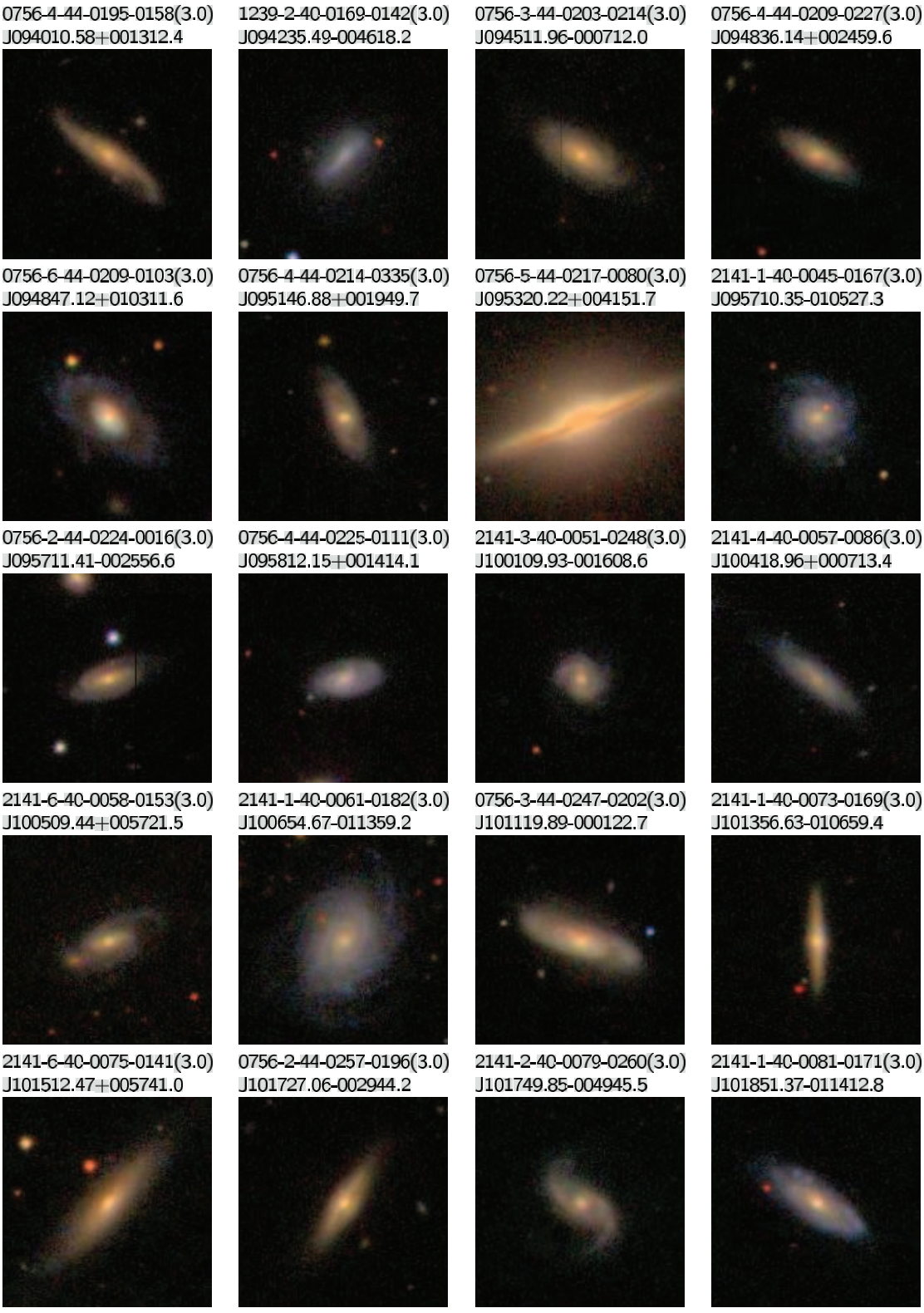

FIG. 6.—Sample of Sb ($T = 3$) galaxies. The format is the same as for Fig. 3.

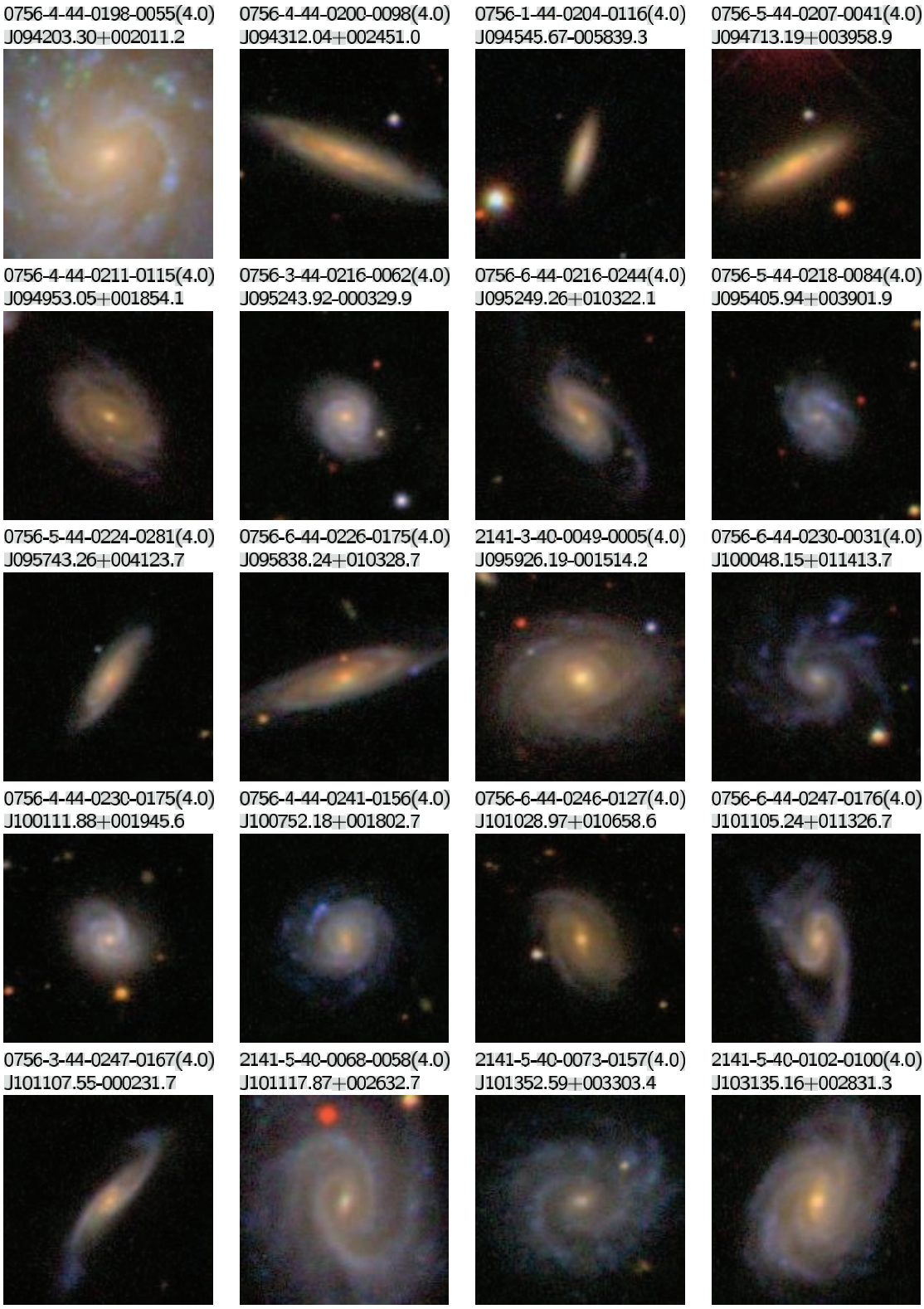

FIG. 7.—Sample of Sc ($T = 4$) galaxies. The format is the same as for Fig. 3.

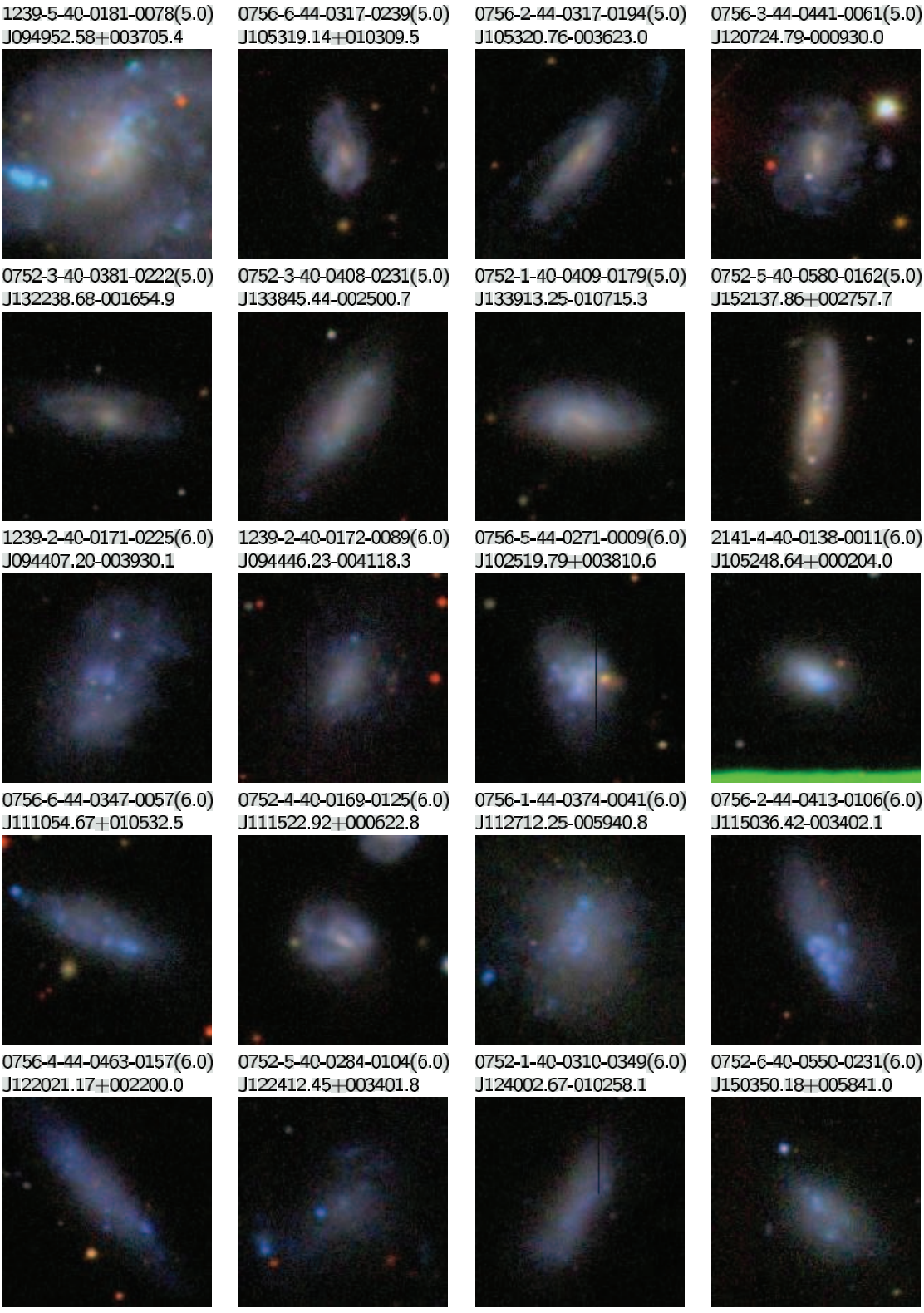

FIG. 8.—Sample of Sd ($T = 5$) and Im ($T = 6$) galaxies. The top two rows display Sd galaxies, and the bottom three display Im galaxies. The format is the same as for Fig. 3.

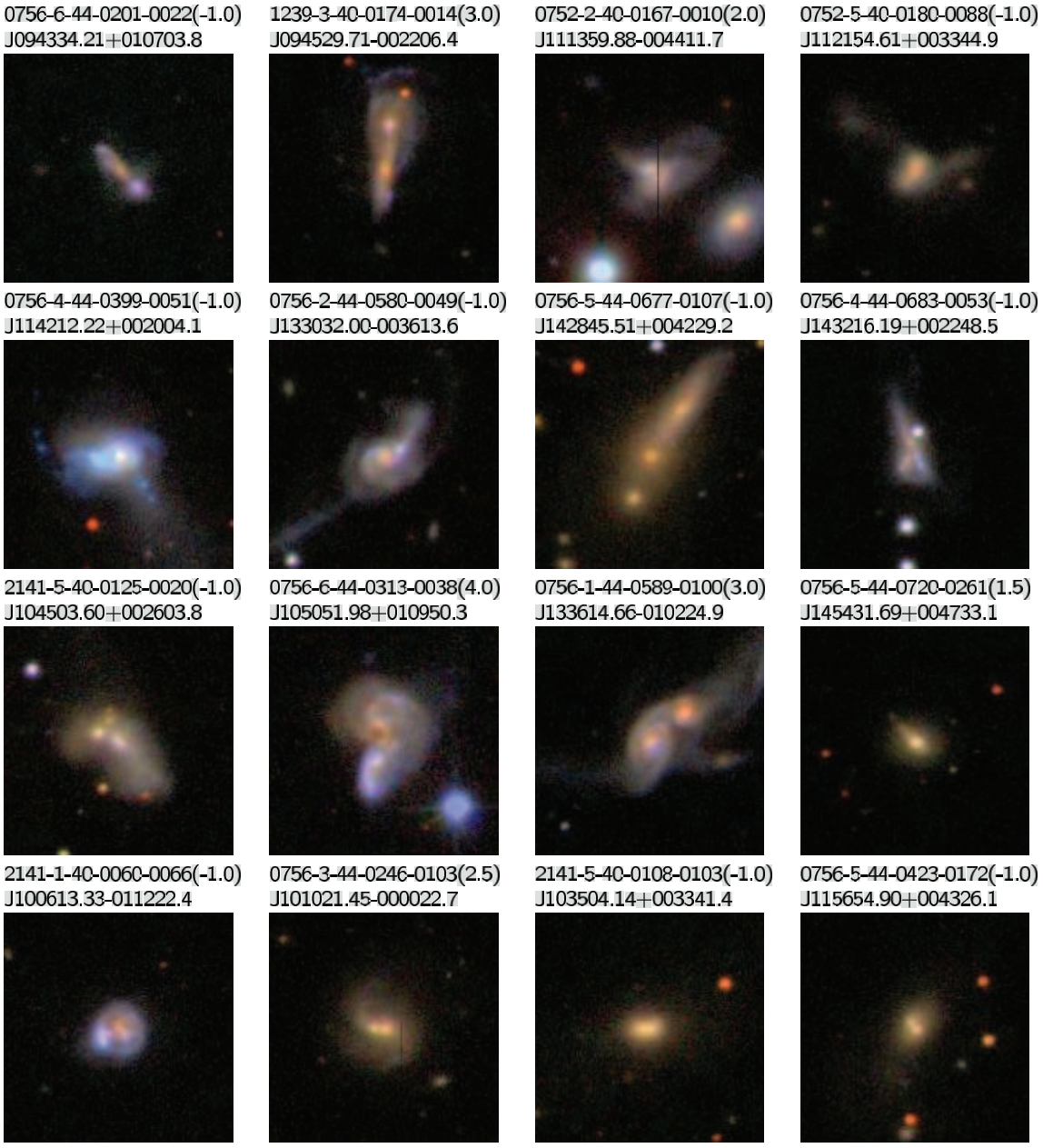

FIG. 9.—Sample of interacting galaxies. The four galaxies in the bottom row are galaxies with double nuclei. The format is the same as for Fig. 3.

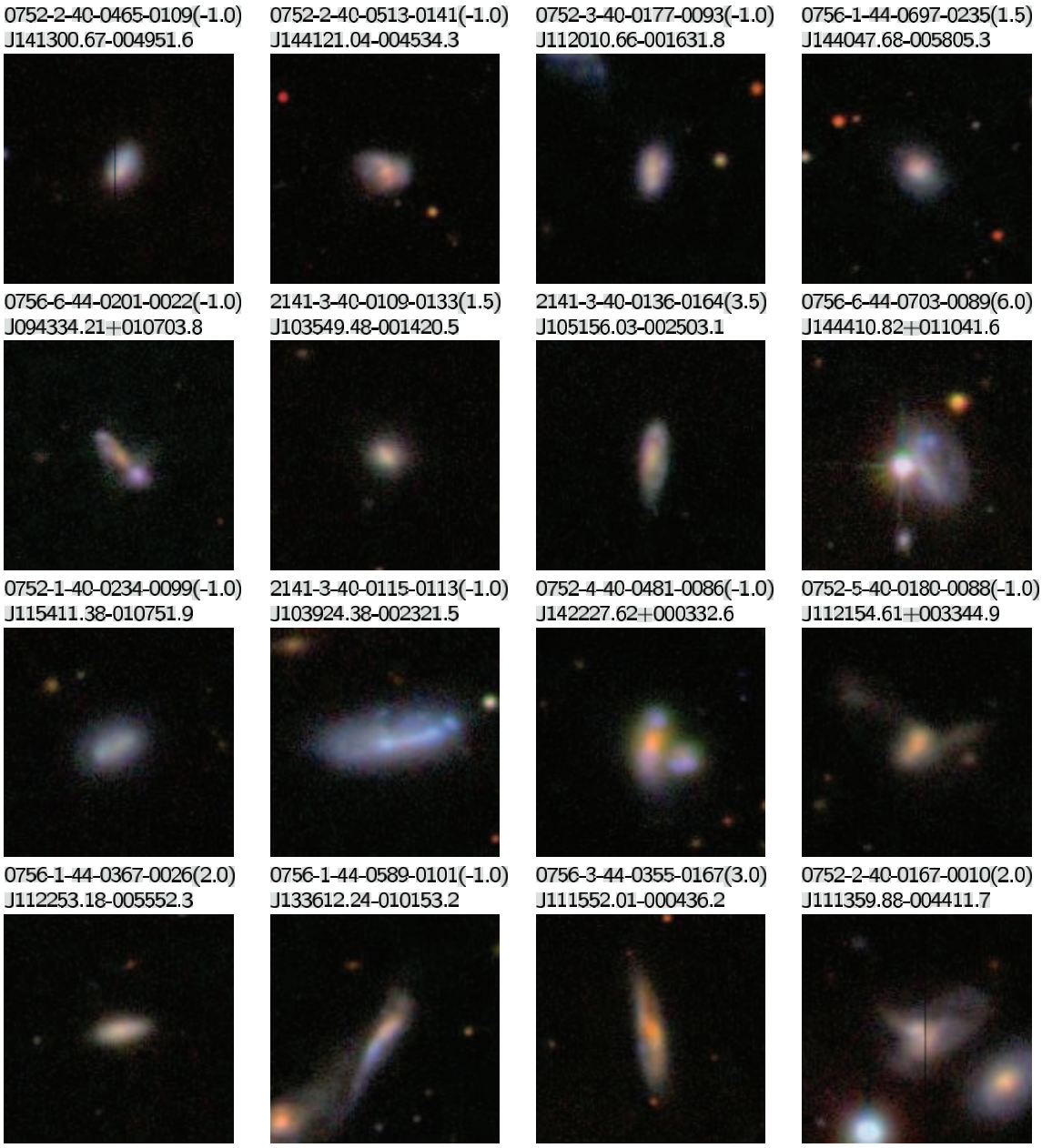

FIG. 10.—Sample of galaxies with amorphous appearance. The format is the same as for Fig. 3.

early-type galaxies are included (see Fig. 2 of Nakamura et al. 2003). This may cause a slight deviation from the smooth $10^{0.6r}$ growth.

An additional test is carried out for the completeness by comparing galaxies in our sample with those in the RC3 and Updated Zwicky Catalogues (Falco et al. 1999). The RC3 contains 269 galaxies in our survey area; 15 of these are not in our catalog. Nine of the 15 are too faint to use ($r > 16$), and two are omitted because they lie too close to the edge of our area. Three (PGC 33550, PGC 39695, and PGC 39705) are in the field for which the SDSS photometric pipeline could not process the frame due to the presence of excessively bright stars (for the first two) or the bright galaxy itself (PGC 33550, $B_T = 9.8$). Another one (PGC 53499 = NGC 5792) is a bright galaxy but lies too close to a very bright star. In summary, only four of 258 RC3 galaxies that should have been included in our catalog were missed.

TABLE 3
NUMBERS OF OBJECTS

Galaxy Sample	Galaxy	Double Counted	Star/Spurious	Initial Sample
Photometric sample	2253	27	378	2658
Targeted spectroscopic sample	2213	20	168	2401
Observed spectroscopic sample	1866	0	18	1884

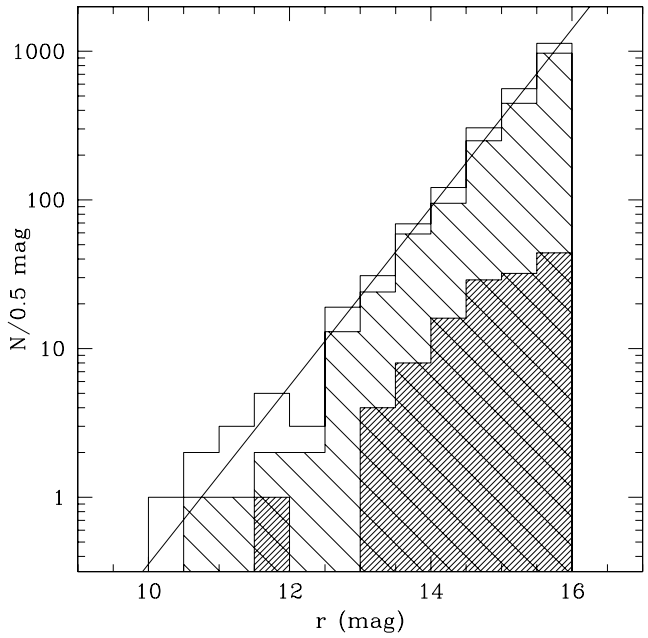

FIG. 11.—Number of galaxies in our catalog per 0.5 mag as a function of r mag. The spectroscopic sample is shown with hatching. Galaxies that carry a flag for photometric errors are indicated by heavy hatching. The curve shows Euclidean growth, $N \sim 10^{0.6r}$.

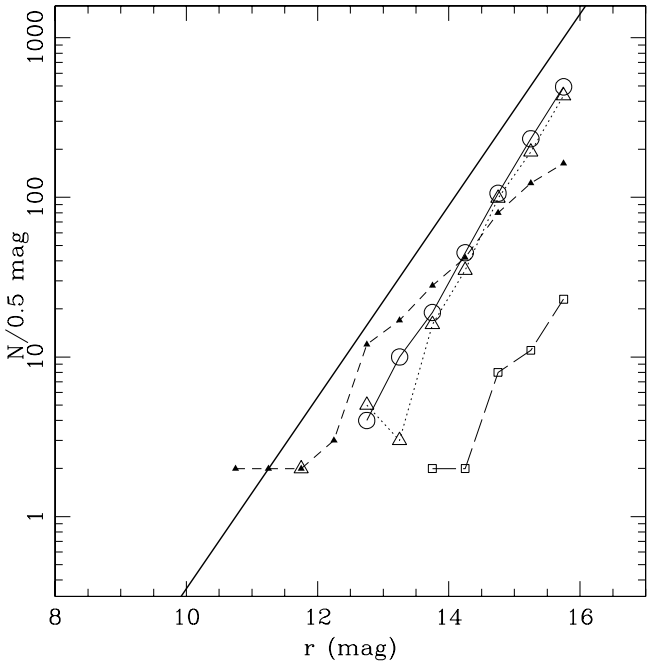

FIG. 12.—Same as Fig. 11, but for each type. Points with $N \geq 2$ are plotted. Circles, open triangles, filled triangles, and squares indicate $T = 0$–1, 1.5–3, 3.5–5, and 5.5–6, respectively. The thick solid line denotes the line of $N \sim 10^{0.6r}$ shown in Fig. 11.

A similar result was obtained in a comparison of the 394 updated Zwicky Catalogue objects in our survey area; 14 of these objects were missed. One Zwicky galaxy (one of a pair of interacting galaxies) was shredded by the deblender into components that all had $r > 16$, and hence were dropped from our catalog. In total, four bright Zwicky galaxies (there are three in common with those we found for the case of RC3) that should have been in our catalog were missed by the SDSS photometric pipeline.

From these tests we conclude that galaxies are well sampled to as bright as 10 mag unless they are accidentally located close to very bright stars. The most important cause of missing bright galaxies is a failure of deblending in the presence of very bright stars or galaxies themselves; we missed a fraction of the region $\approx 1.3 \times 10^{-4}$. We expect that the incompleteness will become an important issue for $r \lesssim 10$. A comparison with the RC3 catalog (which includes all Zwicky galaxies) shows that incompleteness for low surface brightness galaxies is no more than that in RC3.

5. STATISTICS

Figure 13 shows histograms of the morphological type distribution of galaxies for both photometric and spectroscopic samples. We use only seven classes, grouping half those classified into half-integer T into each adjoining integer bin. The fractional morphological composition of our catalog breaks down to E:E/S0-S0:S0a-Sab:Sb-Sc:Scd-Sdm:Im = 0.14:0.26:0.25:0.28:0.038:0.014. A B-band study summarized by Fukugita et al. (1998) gave a relative frequency of E:S0:Sab:Sbc:Scd:Im = 0.11:0.21:0.28:0.29:0.045:0.061. A somewhat higher fraction of early-type galaxies in our sample is ascribed to our galaxy selection in the r band, which will select a larger fraction of early-type galaxies than would be present in a volume-limited sample. Our small fraction of Im galaxies arises from the intrinsic small luminosity of these sources, which makes the sampling volume small. These issues are discussed in Nakamura et al. (2003), where the morphologically classified luminosity function is derived.

We identified 25 galaxies that are interacting, and an additional six that display features that suggest interaction. Of this set of 31, 16 have such disturbed morphologies that they are assigned $T = -1$ (unclassified). In our galaxy sample 12 galaxies have double (or multiple) nuclei, and four of these are also counted as "interacting" and one as a suspected interacting galaxy. Adding double-nucleus galaxies, we arrive at 33–38 interacting galaxies in our catalog; i.e., the rate of interacting galaxies in a nearby magnitude-limited galaxy sample is 1.5%–1.7%.

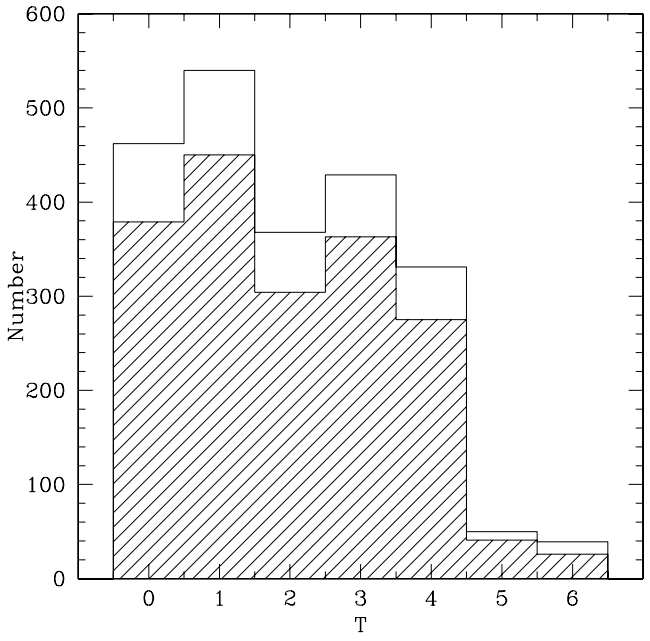

FIG. 13.—Distribution of the morphological types in the galaxy sample selected with $r \leq 16$. Galaxies with half-integer T indices are grouped into each adjoining integer bin. Hatching represents the spectroscopic sample.

TABLE 4
STATISTICAL PROPERTIES OF GALAXIES

Color	E	S0	Sa	Sb	Sc	Sd	Im
Total number	265	255	139	188	166	9	18
$u-g$	1.73 ± 0.18	1.65 ± 0.21	1.50 ± 0.29	1.33 ± 0.28	1.35 ± 0.26	1.18 ± 0.10	1.15 ± 0.34
$g-r$	0.77 ± 0.04	0.74 ± 0.07	0.68 ± 0.10	0.60 ± 0.13	0.54 ± 0.10	0.47 ± 0.09	0.36 ± 0.13
$r-i$	0.39 ± 0.03	0.38 ± 0.04	0.35 ± 0.05	0.31 ± 0.09	0.26 ± 0.08	0.16 ± 0.08	0.09 ± 0.11
$i-z$	0.18 ± 0.04	0.19 ± 0.05	0.18 ± 0.07	0.15 ± 0.09	0.06 ± 0.13	0.01 ± 0.15	-0.06 ± 0.21

NOTES.—Those galaxies that are classified as a half-integer type are omitted from these statistics. The error stands for the dispersion.

The mean colors of galaxies after k-correction (Blanton et al. 2003b) are given in Table 4. We have rejected galaxies for which poor photometry is suspected ($I_{\rm ph} \geq 2$). This information supersedes the mean colors given in Shimasaku et al. (2001).[13] The colors, except for $i-z$, form monotonic sequences from red to blue with increasing T, including half-integer types that are not shown in this table. The scatter of colors among different galaxies at given T is larger than the difference between the mean colors of the neighboring types. For example, the mean colors of E galaxies for $u-g$, $g-r$, and $r-i$ are within 1 σ of those of Sa galaxies. The $i-z$ colors stay essentially constant from E to Sab. For later types, some bluing trend is present in $i-z$, but the scatter widens and is larger than the variation. The mean colors of E galaxies are $u-g=1.73 \pm 0.18$ (1.99), $g-r=0.77 \pm 0.04$ (0.77), $r-i=0.39 \pm 0.03$ (0.43), and $i-z=0.18 \pm 0.04$ (0.36), where the numbers in parentheses are the spectrosynthetic calculation of Fukugita et al. (1995). There is a significant disagreement in the reddest colors, as was noted by Shimasaku et al. (2001).

[13] Shimasaku et al. (2001) did not include k-corrections due to a lack of redshift at that time. Although the galaxies are all at low redshift, the absence of k-corrections make galaxies, especially those of early types, redder by a non-negligible amount. Without the k-correction the colors quoted below in this paragraph will be 1.85, 0.89, 0.41, and 0.28 for the sample used in the present paper.

This work was supported in Japan by Grant-in-Aid of the Ministry of Education. M. F. received support from the Monell Foundation at the Institute for Advanced Study. Funding for the SDSS and SDSS-II has been provided by the Alfred P. Sloan Foundation, the Participating Institutions, the National Science Foundation, the US Department of Energy, the National Aeronautics and Space Administration, the Japanese Monbukagakusho, the Max Planck Society, and the Higher Education Funding Council for England. The SDSS Web site is http://www.sdss.org. The SDSS is managed by the Astrophysical Research Consortium for the Participating Institutions. The Participating Institutions are the American Museum of Natural History, the Astrophysical Institute Potsdam, the University of Basel, Cambridge University, Case Western Reserve University, the University of Chicago, Drexel University, Fermilab, the Institute for Advanced Study, the Japan Participation Group, Johns Hopkins University, the Joint Institute for Nuclear Astrophysics, the Kavli Institute for Particle Astrophysics and Cosmology, the Korean Scientist Group, the Chinese Academy of Sciences, Los Alamos National Laboratory, the Max Planck Institute for Astronomy, the Max Planck Institute for Astrophysics, New Mexico State University, Ohio State University, the University of Pittsburgh, the University of Portsmouth, Princeton University, the US Naval Observatory, and the University of Washington.

REFERENCES

Abazajian, K., et al. 2003, AJ, 126, 2081
———. 2004, AJ, 128, 502
———. 2005, AJ, 129, 1755
Adelman-McCarthy, J. K., et al. 2006, ApJS, 162, 38
Ball, N. M., Loveday, J., Fukugita, M., Nakamura, O., Okamura, S., Brinkmann, J., & Brunner, R. J. 2004, MNRAS, 348, 1038
Blanton, M. R., Lin, H., Lupton, R. H., Maley, F. M., Young, N., Zehavi, I., & Loveday, J. 2003a, AJ, 125, 2276
Blanton, M. R., et al. 2003b, AJ, 125, 2348
———. 2005, AJ, 129, 2562
de Vaucouleurs, G., & de Vaucouleurs, A. 1964, Reference Catalogue of Bright Galaxies (Austin: Univ. Texas Press)
de Vaucouleurs, G., de Vaucouleurs, A., Corwin, H. G., Buta, R. J., Paturel, G., & Fouqué, P. 1995, Third Reference Catalogue of Bright Galaxies (New York: Springer) (RC3)
Driver, S. P., et al. 2006, MNRAS, 368, 414
Falco, E. E., et al. 1999, PASP, 111, 438
Fukugita, M., Hogan, C. J., & Peebles, P. J. E. 1998, ApJ, 503, 518
Fukugita, M., Ichikawa, T., Gunn, J. E., Doi, M., Shimasaku, K., & Schneider, D. P. 1996, AJ, 111, 1748
Fukugita, M., Nakamura, O., Turner, E. L., Helmboldt, J., & Nichol, R. C. 2004, ApJ, 601, L127
Fukugita, M., Shimasaku, K., & Ichikawa, T. 1995, PASP, 107, 945
Gallagher, J. S., & Hunter, D. A. 1987, AJ, 94, 43
Gunn, J. E., et al. 1998, AJ, 116, 3040
———. 2006, AJ, 131, 2332
Hogg, D. W., Finkbeiner, D. P., Schlegel, D. J., & Gunn, J. E. 2001, AJ, 122, 2129
Kochanek, C. S., et al. 2001, ApJ, 560, 566
Lahav, O., et al. 1995, Science, 267, 859
Lupton, R. H. 2006, AJ, submitted
Marzke, R. O., Geller, M. J., Huchra, J. P., & Corwin, H. G. 1994, AJ, 108, 437
Nakamura, O., Fukugita, M., Brinkmann, J., & Schneider, D. P. 2004, AJ, 127, 2511
Nakamura, O., Fukugita, M., Yasuda, N., Loveday, J., Brinkmann, J., Schneider, D. P., Shimasaku, K., & SubbaRao, M. 2003, AJ, 125, 1682
Nilson, P. 1973, Uppsala General Catalogue of Galaxies (Uppsala: Astron. Obs.)
Ohama, N. 2003, Master's thesis, Univ. Tokyo
Pier, J. R., Munn, J. A., Hindsley, R. B., Hennessy, G. S., Kent, S. M., Lupton, R. H., & Ivezić, Ž. 2003, AJ, 125, 1559
Sandage, A. 1961, The Hubble Atlas of Galaxies (Washington: Carnegie Inst.)
Sandage, A., & Brucato, R. 1979, AJ, 84, 472
Sandage, A., & Tammann, G. A. 1980, A Revised Shapley-Ames Catalog of Bright Galaxies (Washington: Carnegie Inst.)
Schlegel, D. J., Finkbeiner, D. P., & Davis, M. 1998, ApJ, 500, 525
Shimasaku, K., et al. 2001, AJ, 122, 1238
Smith, J. A., et al. 2002, AJ, 123, 2121
Stoughton, C., et al. 2002, AJ, 123, 485
Strauss, M. A., et al. 2002, AJ, 124, 1810
Tasca, L. A. M., & White, S. D. M. 2005, preprint (astro-ph/0507249)
Yamauchi, C., et al. 2005, AJ, 130, 1545
York, D. G., et al. 2000, AJ, 120, 1579